Article:
Ashcroft, A.E., Brinker, A., Coyle, J.E. et al. (8 more authors) (2002) Structural Plasticity and Noncovalent Substrate Binding in the GroEL Apical Domain. A study using electrospray ionization mass spectrometry and fluorescence binding studies. Journal of Biological Chemistry, 277 (36). 33115-33126. ISSN 1083-351X

https://doi.org/10.1074/jbc.M203398200

THE JOURNAL OF BIOLOGICAL CHEMISTRY
Vol. 277, No. 36, Issue of September 6, pp. 33115–33126, 2002

Printed in U.S.A.

Structural Plasticity and Noncovalent Substrate Binding in the GroEL Apical Domain

A STUDY USING ELECTROSPRAY IONIZATION MASS SPECTROMETRY AND FLUORESCENCE BINDING STUDIES*

Received for publication, April 9, 2002, and in revised form, June 12, 2002
Published, JBC Papers in Press, June 13, 2002, DOI 10.1074/jbc.M203398200

Alison E. Ashcroft,[a,b] Achim Brinker,[c,d] Joseph E. Coyle,[a,e] Frank Weber,[c,f] Markus Kaiser,[g] Luis Moroder,[g] Mark R. Parsons,[a] Joachim Jager,[a,h] Ulrich F. Hartl,[c] Manajit Hayer-Hartl,[c] and Sheena E. Radford[a,i]

From the [a]Astbury Centre for Structural Molecular Biology & School of Biochemistry & Molecular Biology, The University of Leeds, Leeds LS2 9JT, United Kingdom, the [c]Department of Cellular Biochemistry, Max Planck Institute for Biochemistry, Am Klopferspitz 18a, D-82152 Martinsried, Germany, and the [g]Department of Bioorganic Chemistry, Max Planck Institute for Biochemistry, Am Klopferspitz 18a, D-82152 Martinsried, Germany

Advances in understanding how GroEL binds to non-native proteins are reported. Conformational flexibility in the GroEL apical domain, which could account for the variety of substrates that GroEL binds, is illustrated by comparison of several independent crystallographic structures of apical domain constructs that show conformational plasticity in helices H and I. Additionally, ESI-MS indicates that apical domain constructs have co-populated conformations at neutral pH. To assess the ability of different apical domain conformers to bind co-chaperone and substrate, model peptides corresponding to the mobile loop of GroES and to helix D from rhodanese were studied. Analysis of apical domain-peptide complexes by ESI-MS indicates that only the folded or partially folded apical domain conformations form complexes that survive gas phase conditions. Fluorescence binding studies show that the apical domain can fully bind both peptides independently. No competition for binding was observed, suggesting the peptides have distinct apical domain-binding sites. Blocking the GroES-apical domain-binding site in GroEL rendered the chaperonin inactive in binding GroES and in assisting the folding of denatured rhodanese, but still capable of binding non-native proteins, supporting the conclusion that GroES and substrate proteins have, at least partially, distinct binding sites even in the intact GroEL tetradecamer.

Several classes of molecular chaperones assist in the folding of newly synthesized polypeptides by preventing off-pathway reactions that lead to aggregation (1–3). The so-called chaperonins (4) are large cylindrical structures that transiently enclose a partially folded polypeptide and allow it to continue folding in a sequestered environment, blocking intermolecular associations between chains during folding. The chaperonin of *Escherichia coli*, GroEL, belongs to the group I class of chaperonins and has been studied in great detail (*e.g.* Refs. 5 and 6). GroEL interacts with an estimated 10–15% of newly synthesized polypeptides in the bacterial cytosol (7, 8).

GroEL is a homotetradecamer of ~57-kDa subunits that are arranged as two heptameric rings stacked back-to-back (9, 10). GroEL requires the presence of a co-chaperone, GroES, together with a controlled cycle of nucleotide binding and hydrolysis, to complete its functional cycle (1, 11, 12). GroES is a single heptameric ring of identical ~10-kDa subunits that binds in a nucleotide-dependent manner to one end of the GroEL cylinder. A substrate protein binds with highest affinity to the nucleotide-free state of GroEL (reviewed in Ref. 1). On subsequent binding of 7 ATP and GroES, the substrate protein is jettisoned into a *cis*-folding cage where it is free to fold to its final native form. Whereas the nucleotide-coupled interplay between GroEL, GroES, and protein substrate is understood in great detail, precisely how GroEL binds a wide array of non-native proteins and assists their folding remains elusive.

Each GroEL subunit consists of an equatorial, an apical, and an intermediate domain (9, 10). The equatorial domains of the subunits contain the ATP-binding site and both the N and C termini; they also mediate most inter-subunit contacts within and between rings. The apical domains form the entrance to the GroEL cavity and contain the residues involved in protein and GroES binding (13). Each intermediate domain forms a hinge-like connector between the equatorial and apical domains of that subunit. Studies of polypeptide recognition by GroEL using various techniques (reviewed in Ref. 14) suggest that the binding site involves the apical domains; more recent crystallographic studies suggest that helices H and I within the apical domain form the substrate-binding site (15–20). Interestingly, these helices are the least well defined regions in the GroEL crystal structure and have relatively high thermal parameters (B-factors) even in the isolated apical domain (21, 22), raising the possibility that the ability of GroEL to bind a diverse range of polypeptides may involve this conformational plasticity. Structural mobility and exposed hydrophobic sur-

* This work was supported by the Astbury Centre for Structural Molecular Biology, part of the Biotechnology and Biological Sciences Research Council (BBSRC) supported by the North of England Structural Biology Centre, and the University of Leeds. The Platform II mass spectrometer was purchased with funds from the Wellcome Trust. The costs of publication of this article were defrayed in part by the payment of page charges. This article must therefore be hereby marked "*advertisement*" in accordance with 18 U.S.C. Section 1734 solely to indicate this fact.

The atomic coordinates and structure factors (code 1LA1) have been deposited in the Protein Data Bank, Research Collaboratory for Structural Bioinformatics, Rutgers University, New Brunswick, NJ (http://www.rcsb.org/).

[b] Supported by the Wellcome Trust.

[d] Supported by Boehringer Ingelheim. Present address: Dept. of Chemistry, The Scripps Research Institute, 10550 North Torrey Pine Rd., La Jolla, CA 92037.

[e] Supported by the BBSRC. Present address: Anadys Pharmaceuticals Inc., San Diego, CA 92121.

[f] Present address: Dept. of Cell Biology, The Scripps Research Institute, 10550 North Torrey Pine Rd., La Jolla, CA 92037.

[h] Supported by the Yorkshire Cancer Research.

[i] BBSRC Professorial Fellow. To whom correspondence should be addressed. Tel.: 113-343-3170; Fax: 113-343-3167; E-mail: s.e.radford@leeds.ac.uk.

faces are features common to both the apical domains of GroEL and non-native polypeptides.

Here we investigate the properties of the apical domain from GroEL and its peptide binding characteristics using a range of analytical techniques. Specifically, the ability of electrospray mass spectrometry (ESI-MS) to simultaneously observe different protein conformations in solution was exploited to study the conformational dynamics of the GroEL apical domain and the ability of different conformers to bind peptide mimics of the co-chaperone GroES and the substrate protein, rhodanese. Parallel fluorescence emission studies were used to study these complexes and compare the binding properties of the apical domain constructs for each peptide with those of intact GroEL. The data suggest that the apical domain possesses different binding sites for the peptides in that no competition for binding individual peptides to the apical domain was observed. Finally, using surface plasmon resonance and fluorescence studies on a GroEL variant in which the GroES-binding groove is blocked by a covalently bound peptide, we show that the substrate and the GroEL mobile loop-binding sites are at least partially distinct even in the intact GroEL tetradecamer.

EXPERIMENTAL PROCEDURES

GroEL and Apical Domain Constructs of GroEL—The apical domain constructs: ApEL[1] (GroEL-(191–376)), N-His ApEL (GroEL-(191–376) containing an N-terminal hexahistidine tag), C-His ApEL (GroEL-(188–381) containing a C-terminal hexahistidine tag), and ApTrap (ApEL G337S/I349E) were cloned, expressed, and purified as described previously (23, 24). The concentration of all apical domain constructs was determined using an extinction coefficient of 4260 M^{-1} cm^{-1} at 280 nm, calculated by the method of Pace *et al.* (25). Wild-type GroEL and EL N229C (intact GroEL containing the mutation N229C and in which all the endogenous cysteine residues have been exchanged for alanine) were purified as described previously (26).

Crystallization—All crystallization screens were performed by vapor diffusion using the hanging drop method at 18 °C. Sparse matrix screens were used to perform initial crystallization trials in 24-well plates with a well volume of 500 μl (27). Lyophilized C-His ApEL was dissolved in, and extensively dialyzed against, buffer (20 mM Tris-HCl, 1 mM DTT, pH 7.2) prior to screening. The final protein solution was 10 mg ml^{-1}. Hanging drops contained equal volumes (2 μl each) of the protein and well solutions. Crystals of C-His ApEL were obtained after 1–2 weeks with a well solution of 0.6 M NaCl, 14% (w/v) PEG 6000, 100 mM Tris-HCl, pH 8.5.

X-ray Data Collection and Structure Determination—Crystals of C-His ApEL were transferred to a solution of mother liquor containing 15% (v/v) glycerol as a cryoprotectant and rapidly frozen in liquid nitrogen prior to data collection. X-ray data were collected using a 30-cm MAR Research image plate detector at the Synchrotron Radiation Source Station 9.6 (Daresbury, UK) (λ = 0.87 Å). Indexing and extraction of the raw x-ray intensities were performed using the program MOSFLM (28). Intensities were merged and amplitudes were calculated using programs from the CCP4 program suite (29). Molecular replacement was carried out with the program AMORE (30) using an initial search model consisting of residues 188–381 from the refined GroEL tetradecamer (21). The high resolution structure of an apical domain fragment closely resembling our construct, containing GroEL residues 191–376 and an N-terminal histidine tag sequence (22), was used subsequently as a model for further modeling and refinement. Initial model building was carried out with the program FRODO (31, 32) and the structure was refined first at medium resolution using X-PLOR (33). Inspection of the resulting model using the program O (34) and full refinement at high resolution including all data was performed using the programs CNS (35) and REFMAC (36).

Helix D and Mobile Loop Synthesis—The peptides helix D (HD) of rhodanese (amino acid residues 248–267) (37) (HD: Ac-RKGVTACHIA-LAAYLCGKPD-NH_2) and mobile loop (ML) of GroES (amino acid residues 13–32) (ML: Ac-KRKEVETKSAGGIVLTGSAA-NH_2) were chemically synthesized with a C-terminal amide on an automated peptide synthesizer (Applied Biosystems, Foster City, CA, model 430A) using standard Fmoc methodology and purified by reverse phase high performance liquid chromatography. The N terminus was modified with either an acetyl or dansyl group, the latter to provide a sensitive fluorescent probe for monitoring binding to the apical domain. The purity and molecular masses of the peptides were verified by analysis of a 10 ng μl^{-1} solution in 1:1 (v/v) acetonitrile, 0.05% aqueous formic acid using positive ionization ESI-MS. The concentrations of dansylated peptides were determined using the extinction coefficient for a single dansyl group of 4500 M^{-1} cm^{-1} at 330 nm (38). The concentrations of non-dansylated peptides were estimated by dry weight.

Electrospray Ionization Mass Spectrometry—The apical domain constructs were analyzed at a concentration of 20 μM by continuous infusion at a flow rate of 5 μl min^{-1} into the electrospray ionization source of a Platform II (Micromass UK Ltd., Manchester, United Kingdom) single quadrupole mass spectrometer using a syringe pump (model 22, Harvard Apparatus, Holliston, MA). Where "native" electrospray conditions were used, the samples were dissolved in ammonium acetate (50 mM) at pH 7.5. Where "denaturing" electrospray conditions were used, the samples were analyzed in 1:1 (v/v) 0.1% aqueous formic acid, acetonitrile. In both cases the ionization source was maintained at 30 °C and nitrogen was employed as both the nebulizing and drying gases at flow rates of 20 and 200 l h^{-1}, respectively. Positive ionization electrospray was used with a capillary voltage of 2.3 kV, the counter electrode set at 0 kV, and the sampling cone at 30 V. Data were acquired over the range m/z 500–3000 at a scan speed of 10 s and processed using MassLynx software (Micromass UK Ltd.). An external calibration using horse heart myoglobin (molecular mass 16,951.5 Da; Sigma) was applied to ensure mass accuracy.

The m/z spectra displayed were smoothed mildly using a Sovitzy-Golay algorithm. The molecular mass (zero charge state) profiles illustrated were generated from the m/z spectra using the Maximum Entropy (39) software supplied with MassLynx.

Thermal Stability of the Apical Domain Constructs Monitored by ESI-MS—To determine the thermal stability of the apical domain constructs, the ionization source temperature was raised in a stepwise fashion from 30–190 °C.

Apical Domain and Peptide Complex Formation Monitored by ESI-MS—The apical domain was mixed with the peptides HD or ML in ammonium acetate (50 mM) at pH 7.5 and the mixtures were incubated for 1 h at ambient temperature prior to ESI-MS analysis. The concentration of the apical domain was maintained at a constant 20 μM although the concentration of ML was varied from 1 to 200 μM and the concentration of HD was maintained at 50 μM to maximize the proportion of the complex without incurring problems with aggregation. The ionization source temperature was maintained at 30 °C and the sampling cone voltage at 30 V; these conditions were chosen to preserve protein-peptide complexation.

Synthesis of SBP-Mal—*N*-Hydroxysuccinimido maleoyl-β-alaninate (Mal>β-Ala-OSu) was prepared following a previously published procedure (40). The precursor peptide Ac-SWMTTPWGFLHP (the so-called strong-binding peptide, SBP (19)) was synthesized with an automated peptide synthesizer (Applied Biosystems model 430A) using standard Fmoc/*t*Bu chemistry on pre-loaded Fmoc-Lys(Boc)-2-chlorotritylresin (loading: 0.62 mmol g^{-1}, 194 mg, 0.12 mmol). After cleavage and deprotection of the peptide with 95:2:3 (v/v/v) trifluoroacetic acid:water:triisopropyl silane and precipitation with methyl *t*-butylether, the precipitate was dissolved in 4:1 (v/v) *t*-butanol:water and lyophilized to produce a yield of 162 mg. The crude product (62 mg) was dissolved in *N*,*N*-dimethylformamide (20 ml) and reacted overnight with Mal>β-Ala-OSu (10.5 mg) and diisopropylethylamine (20.3 μl). After evaporation, the residue was dissolved in 4:1 (*v/v*) *t*-butanol:water and lyophilized. The resulting product was purified on a Nucleosil™ C_{18} column using a linear gradient of 30–80% (v/v) aqueous acetonitrile in 60 min. The product-containing fractions were pooled and the solution was dried. The residue was dissolved in 4:1 (v/v) *t*-butanol:water and lyoph-

[1] The abbreviations used are: ApEL, GroEL (residues 191–376); ApTrap, ApEL containing the mutations G337S and I349E; HD, helix D; ML, mobile loop; C-His ApEL, GroEL (residues 188–381) with a C-terminal hexahistidine tag; N-His ApEL, GroEL (residues 191–376) with an N-terminal hexahistidine tag; SBP-Mal, strong binding peptide with a C-terminal maleimide; EL N229C, intact GroEL containing the mutation N229C and in which all the endogenous cysteine residues have been exchanged for alanine; EL N229C-SBP, intact GroEL containing the mutation N229C and in which all the endogenous cysteine residues have been exchanged for alanine, with the 229C covalently bound to SBP-Mal; GroES 98C, GroES mutant in which a cysteine residue has been added to the C terminus; WT GroEL, wild-type GroEL; Fmoc, *N*-(9-fluorenyl)methoxycarbonyl; DTT, dithiothreitol; dansyl, 5-dimethylaminonaphthalene-1-sulfonyl; MOPS, 4-morpholinepropanesulfonic acid; r.m.s., root mean square.

ilized to yield 12 mg of 98% pure material as verified by high performance liquid chromatography and mass spectrometric analysis.

Modification of GroEL N229C—A ~3-fold molar excess of SBP-Mal over EL N229C cysteines was applied to achieve quantitative modification. SBP-Mal (10 mM in Me_2SO) was diluted 20-fold with H_2O. 200 μl of EL N229C (to give a final concentration 9 μM) was added to 1 ml of 0.5 mM peptide solution and incubated for 1 h at 25 °C. The reaction was stopped by the addition of β-mercaptoethanol (50 mM) and excess reagent was removed by gel filtration chromatography. Less than 10% free thiols were detected in EL N229C:SBP-Mal on treatment with maleimidosalicylic acid.

Prevention of Rhodanese Aggregation—Denatured rhodanese (100 μM in 6 M guanidinium chloride) was diluted 200-fold into buffer (20 mM MOPS, pH 7.4, 100 mM KCl, 5 mM $MgCl_2$) in the absence or presence of 1.0 μM EL N229C or EL N229C:SBP-Mal. Rhodanese aggregation was followed by turbidity measurements at 320 nm.

Steady State Fluorescence—Steady state fluorescence emission was measured at 20 °C on a spectrofluorimeter (model LS50B, PerkinElmer Life Sciences) using a 1-cm path length. Protein-peptide complexes were equilibrated for 5 min prior to acquiring fluorescence emission spectra. Fluorescence emission scans of dansylated peptides were recorded between 450 and 600 nm, using an excitation wavelength of 350 nm and a scan speed of 60 nm min^{-1}. Excitation and emission slit widths were typically between 5 and 10 nm. Peptide binding titrations were performed with similar parameters but in the time drive mode, measuring emission at a single wavelength. The emission wavelength used was 500 nm for HD and 535 nm for ML binding to ApEL, respectively. All titrations were performed by adding small volumes of the dansyl-ML or ApEL to a cuvette containing 2–3 ml of either ApEL (25 mM) or dansyl-HD (3 mM), respectively, in buffer (50 mM Hepes, pH 7.5, 2 mM DTT). After each addition, the solution was mixed thoroughly and allowed to equilibrate thermally for ~5 min. Titration of ApEL with the dansyl-ML required ~25-min equilibration times. The total volume of ligand added never exceeded 10% of the total volume. For each assay, a control experiment was performed by adding the ligand to a solution of buffer alone and was subtracted from the corresponding reading acquired in the presence of protein or peptide.

Fitting of Ligand Binding Data—All peptide binding curves were fitted using the program Grafit™ (Erithacus Software Ltd.). Single transition ligand-binding profiles were fitted with either a weak (Equation 1) or tight (Equation 2) ligand binding equation as appropriate (41). Typically, the weak binding equation was used under conditions where the dissociation constant was greater than the concentration of binding sites and the tight ligand binding equation was used under conditions where the concentration of binding sites was much greater than the dissociation constant.

$$F = \frac{(F_{max}[L])}{K_d + [L]} \quad \text{(Eq. 1)}$$

Where F is the signal, F_{max} is the maximum signal, K_d is the dissociation constant, and L is the concentration of ligand.

$$F = \frac{(E_0 + K_d + L) + ((E_0 + K_d + L)^2 - (4E_0L))^{1/2}}{2E_0} \times [(F_{max} - F_{min})] + F_{min} \quad \text{(Eq. 2)}$$

Where F is the signal, F_{max} and F_{min} are the maximum and minimum signals, respectively, E_0 is the protein ligand-binding site concentration, K_d is the dissociation constant, and L is the total ligand concentration.

Surface Plasmon Resonance—Mutant GroES 98C (42) (mutant cochaperone GroES with an additional cysteine at the C-terminal) was purified as described previously (26) and immobilized (300 resonance units) via a thioether linkage on a CM5 biosensor chip (Biacore 2000 SPR instrument, Biacore AB, Uppsala, Sweden) and the analysis was performed as described previously (43). Binding was followed using buffer (20 mM MOPS, pH 7.4, 100 mM KCl, 5 nM $MgCl_2$, 2 mM ATP) at a flow rate of 20 μl min^{-1} at 25 °C. The concentration of GroEL was 250 nM.

RESULTS

Various GroEL apical domain fragments, mainly spanning amino acids 191–376 (with or without a hexahistidine tag) were expressed and purified for these studies (Fig. 1*A*). ApTrap contains two point mutations in GroEL-(191–376): G337S and I349E, which in intact wild-type (WT) GroEL result in loss of ability of GroEL to release bound polypeptide (13, 44). Additionally, C-His ApEL is a slightly larger apical domain construct, encompassing residues GroEL-(188–381), containing a C-terminal hexahistidine tag.

Crystal Structure Analysis of GroEL Apical Domains—Several crystal structures of GroEL apical domains have been obtained to date (9, 19, 22, 45, 46). To compare the structure of these domains with that of the larger construct C-His ApEL constructed here, crystals of C-His ApEL were grown as described under "Experimental Procedures." Crystals appeared within 1–2 weeks and belong to space group $P2_12_12_1$ with unit cell dimensions of a = 48.6 Å, b = 61.9 Å, and c = 75.2 Å. A 98.8% complete data set was collected at cryogenic temperatures from a single crystal to 2.06-Å resolution. The molecular replacement procedure revealed a clear solution in both the rotation and translation searches. The correlation coefficient corresponding to the highest peak in the translation function was 0.600 and the initial R-factor after rigid-body optimization was 0.387 (47).

The crystal structure of the apical domain fragment, C-His ApEL (residues 188–381), is well defined. The free R of the final refined model is 0.257 including 95% of all data between 20 and 2.06 Å. In the current model the deviations in ideal bond lengths and bond angles were 0.011 Å and 2.4°, respectively, and the average real-space correlation coefficient for all amino acid residues was 0.936. The backbone torsion angles of all residues are within the allowed regions of the Ramachandran plot (data not shown). The overall data collection and model refinement statistics are collated in Table I and the coordinates have been deposited in the Protein Data Bank as 1LA1.

C-His ApEL shares a virtually identical fold to its counterparts in both the intact GroEL tetradecamer as well as in the shorter domains 191–336, 191–345, 193–345, and 191–376 (9, 16, 19, 22, 46). A comparison of five independent models of the apical domain of GroEL, namely C-His ApEL (determined here), N-His ApEL (22), ApEL-(191–336)·peptide complex (19), intact GroEL (9), and a GroEL·ADP complex (45) is shown in Fig. 1*B*. The C-His ApEL model can be superimposed onto equivalent α-carbon atoms in the intact tetradecamer, the high-resolution N-His ApEL model, the ApEL-(191–336)·peptide complex, and the GroEL·ADP complex with overall r.m.s. deviations of 0.72, 0.53, 0.56, and 1.57 Å, respectively. The α-carbon atoms in the β-sandwich core of the ApEL domain are virtually unchanged in the different models. The r.m.s. deviation of the core structure in the C-His ApEL and N-His ApEL models was only 0.32 Å. Similarly, the overlap between the core of the ApEL domains and the equivalent region in the intact EL tetradecamer was 0.65 Å. However, the most striking feature of the structural comparisons was that the local changes were significantly higher and map predominantly to helices H and I. Displacements of up to 2.0 Å can be found in this part of the ApEL domain (Fig. 1*C*). Consistent with previous observations (19, 22, 23) these data suggest that helices H and I, which have been implicated in substrate binding (15–20), are locally dynamic.

ESI-MS of GroEL Apical Domain Constructs—We first investigated the characteristics of ApEL, the wild-type apical domain construct of GroEL (Fig. 1*A*) under varying conditions by ESI-MS analysis. Under denaturing conditions at pH 2 in a 1:1 (v/v) 0.1% aqueous formic acid, acetonitrile, the *m/z* spectrum of ApEL (Fig. 2*A*) shows a single, wide distribution of charge states (n) ranging from n = +10 to +29 consistent with the population of a single conformational species of a pure and highly denatured protein of measured molecular mass 20,239.5 Da (calculated mass 20,239.4 Da).

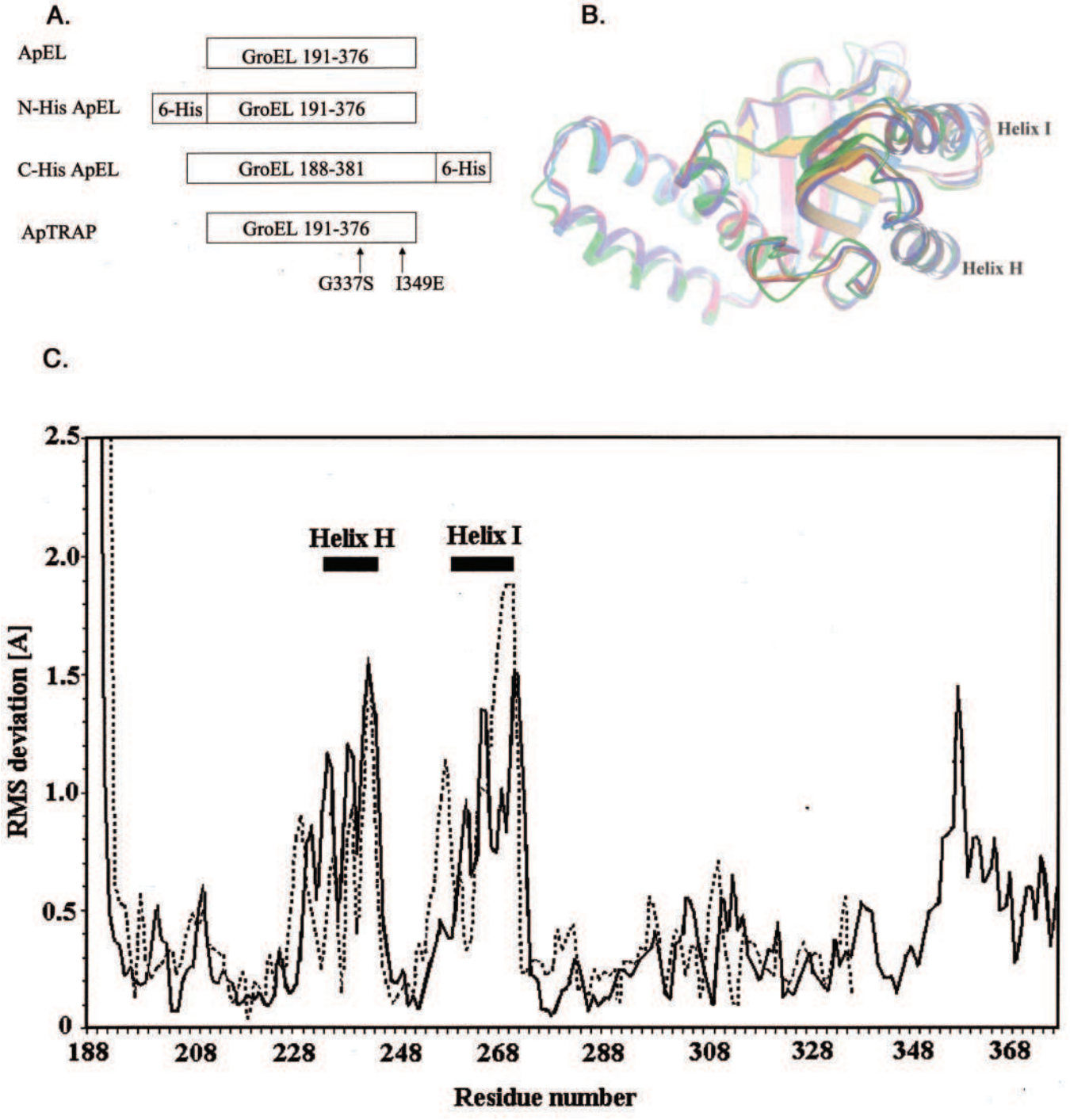

FIG. 1. **Apical domain constructs of GroEL.** *A*, GroEL apical domain constructs indicating the amino acid residues included and modifications made in the proteins expressed for these studies. *B*, ribbon diagram showing a comparison of the overall structures of five independent GroEL apical domains: C-His ApEL (determined here) (*purple*), N-His ApEL (22) (*red*), ApEL-(191–336)·peptide complex (19) (*yellow*), intact WT GroEL (9) (*blue*), and a GroEL·ADP complex (45) (*green*). The diagram shows the conformational flexibility in the region around helices H and I. *C*, r.m.s. deviation plot showing the differences in C-α positions between C-His ApEL and N-His ApEL (22) (*unbroken line*), and C-His ApEL and an ApEL-(191–336)·peptide complex (19) (*dotted line*).

Under native electrospray ionization conditions (50 mM aqueous NH_4OAc, pH 7.5) the *m/z* spectrum of the ApEL construct changes significantly (Fig. 2*B*). The range of charge states is wider (n = +7 to +29) and more complex than anticipated for a folded protein of this molecular mass. Significantly, the number and range of charge state distributions observed is consistent with the protein existing in a number of distinct conformations at this pH. The first distribution, centered on charge state n = +9, represents ~30% of molecules, and suggests that these molecules are tightly folded. A second distribution of charge states is centered on approximately n = +21. These states represent ~60% of the protein molecules, indicating that a substantial proportion of apical domain molecules were expanded relative to the native state, even under neutral pH conditions. Finally, a third charge state distribution centered on n = +13 is observed (~10% of the total protein), corresponding to a third, distinct, population of partially folded molecules. Similar multiple charge state distributions were observed under native conditions for the other apical domain constructs N-His ApEL, C-His ApEL, and ApTrap (data not

shown). These data indicate that the apical domain was conformationally dynamic, co-populating multiple species with distinct properties at neutral pH.

To determine whether the different charge state distributions reflect molecules in rapid equilibrium or distinct conformational states of native and more highly denatured species, the effect of varying the ESI-MS conditions on the charge state distribution of ApEL was investigated. The effect of the sampling cone voltage on the charge state distributions for ApEL at pH 7.5 is shown in Fig. 3*A*. When the cone voltage is increased, the charge states corresponding to the most highly unfolded molecules centered on $n = +21$ shift to higher *m/z* and hence lower charge states, as might be expected for the "charge stripping" phenomenon of proteins observed with increasing sampling cone voltage (48). When the cone voltage is raised above 70 V, the protein signal becomes weaker and the signal to noise ratio decreases, most probably because of sample decomposition and possibly fragmentation under the harsh conditions. In contrast, the charge state distribution corresponding to more folded molecules centered on the $n = +9$ charge state changes little with increasing cone voltage until 190 V, and only then does this particular charge state distribution widen, consistent with partial unfolding at the higher cone voltage. This indicates a remarkable stability of this subset of molecules to cone voltage compared with other native proteins (49). The resistance of this distribution to increases in sampling cone voltage supports the notion that these molecules are natively folded in a stable structure.

In a second series of experiments the stability of ApEL with respect to ionization source temperature was studied (Fig. 3*B*). As described above, at pH 7.5, with an ionization source temperature of 30 °C, multiple charge state series were observed. As the ionization source temperature is increased above 75 °C, however, the proportion of unfolded protein molecules increases although the folded protein population decreases concomitantly. At an ionization source temperature of 150 °C, virtually all of the protein molecules were unfolded. Similar behavior was exhibited by the other apical domain constructs shown in Fig. 1*A* (data not shown). These findings are consistent with the notion that the more highly folded populations of the domain unfold at increased electrospray solution temperature suggesting that the different charge state populations observed at lower temperatures represent distinct conformational states of apical domains that are co-populated and in equilibrium with each other at pH 7.5.

Polypeptide Binding to GroEL Apical Domains—ESI-MS offers a unique opportunity to investigate simultaneously the ability of different conformational species of the GroEL apical domain to bind cofactors and substrates. Two model peptides were selected for such binding studies. The first peptide is equivalent to the mobile loop sequence of GroES (residues 13–32) (50, 51), a region that has been shown to mediate the interaction between GroES and GroEL by binding to the GroEL apical domain between helices H and I in the intact GroEL-GroES structure. This region of GroES has been shown to be

TABLE I
Crystallographic statistics for the apical domain construct C-His ApEL

Crystallographic statistics	Model C-His ApEL$^-$ (188–381)
Unit cell dimensions	$a = 48.6$ Å, $b = 61.9$ Å, $c = 75.2$ Å
Space group	$P2_12_12_1$
Number of reflections (obs./poss.)	14319/15933
Overall completeness	98.8%
Significance $\langle I/\sigma I \rangle$	10.1
Resolution limits	20.0–2.06 Å
No. of non-hydrogen atoms	1448
No. of solvent molecules	447
Crystallographic *R*-factor	0.197
Free *R*-factor	0.257
R.m.s bond	0.011 Å
R.m.s angle	2.4 °
R.m.s. dihedrals	23.90 °

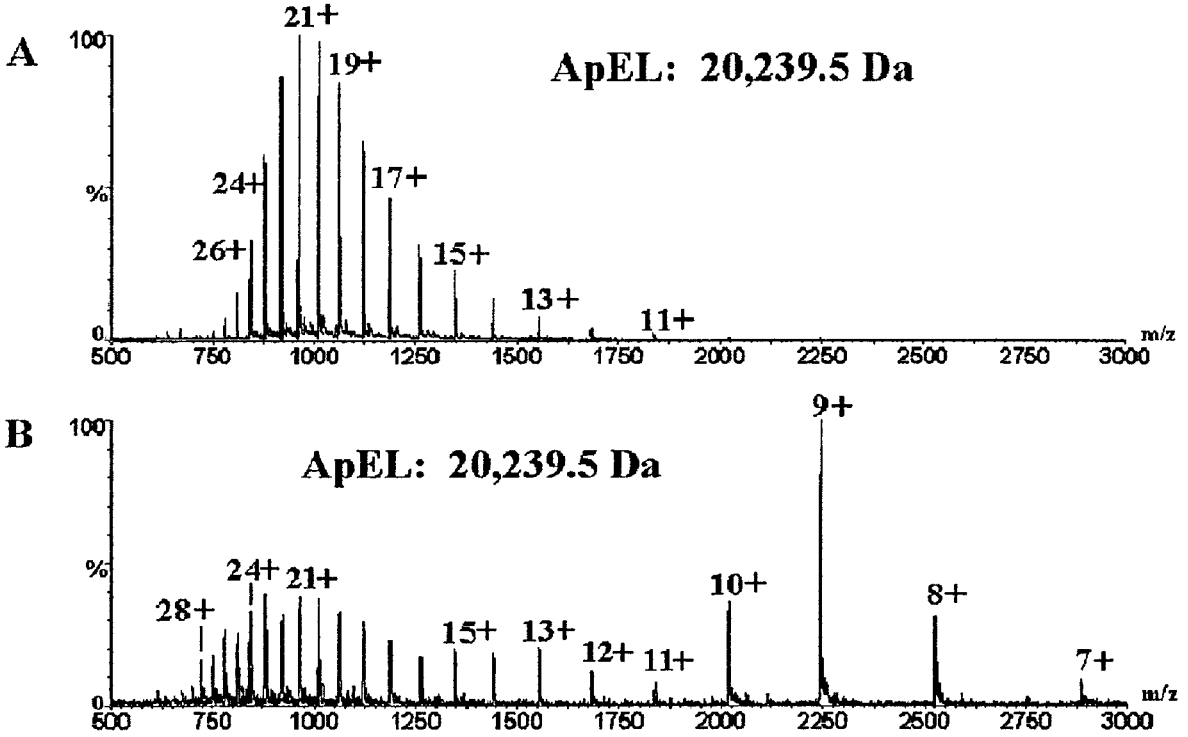

FIG. 2. **ESI-MS *m/z* spectra of ApEL (ionization source temperature of 30 °C).** *A,* at pH 2 in 1:1 (v/v) acetonitrile, 0.1% formic acid, showing a single charge state distribution ($n = +10$ to $+29$; centered on $n = +21$), and *B,* at pH 7.5 in 50 mM aqueous NH_4OAc, showing multiple charge state distributions centered on $n = +9$, $+13$, and $+21$.

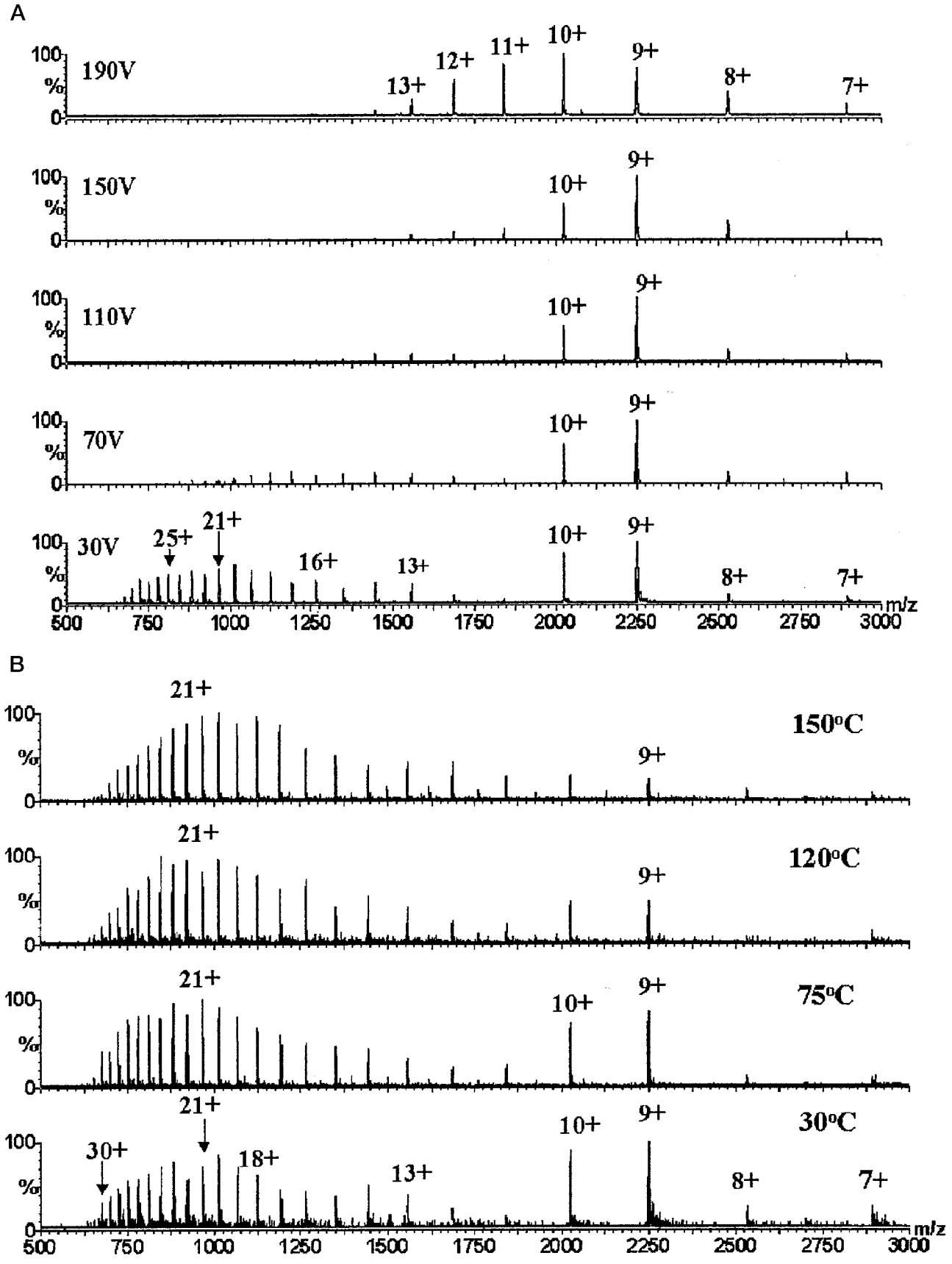

FIG. 3. **ESI-MS *m/z* spectra of ApEL showing the effect of the ionization source temperature and cone voltage on the various conformational states.** *A*, the ESI-MS *m/z* spectra of ApEL analyzed at pH 7.5 in 50 mM aqueous NH_4OAc with an ionization source temperature of 30 °C showing the variation of the charge state distribution with increased sampling cone voltage. The folded population remains stable up to a cone voltage ≥150 V. *B*, the ESI-MS *m/z* spectra of ApEL analyzed at pH 7.5 in 50 mM aqueous NH_4OAc with a sampling cone voltage of 30 V showing the variation of the charge state distribution with increasing ionization source temperatures. The folded population has virtually disappeared at a temperature of 150 °C. Additionally, at the higher temperatures a trace of protein dimerization is also observed.

conformationally dynamic using both NMR (50) and x-ray crystallography (52). Additionally, previous NMR studies have shown that the isolated ML peptide bound to GroEL adopts the same β-hairpin structure as in intact GroES (51).

The second peptide represents helix D of rhodanese, a stringent GroEL substrate. This helical region has been shown to bind to the surfaces of the apical domain in GroEL using cross-linking and proteolysis experiments (53). The HD peptide used in our studies is equivalent to amino acid residues 248–267 of the sequence of intact rhodanese. This region encompasses the native α-helix, together with three flanking residues at the N and C termini to stabilize the helix and to produce a predominantly hydrophobic peptide with a net positive charge to facilitate its solubility. Accordingly, HD was found to be soluble at a concentration of 50 μM at pH 7.5 and ~30% helical as judged by far UV CD (data not shown).

The ability of ApEL to bind ML or HD was first investigated using fluorescence studies. In these experiments, dansylated peptides (see "Experimental Procedures") were added separately to ApEL and the fluorescence emission spectra of the peptides were examined. The data indicate that the fluorescence emission intensities of the dansylated peptides increase (Fig. 4, *A* and *B*) and the λ_{max} shifts to shorter wavelength (data not shown) upon binding of both peptides to the apical domain construct, suggesting that both peptides bind to the apical domains such that the dansyl group is located in a more hydrophobic environment. Titration data show that both peptides bind to ApEL with similar affinity, K_D(ML) = 2.7 ± 0.7 μM and K_D(HD) = 2.2 ± 0.1 μM; their affinity for the apical domain thus lies within the range commonly observed for peptides binding to GroEL (38, 54, 55). Strikingly, both peptides bind with a 1:1 stoichiometry, demonstrating the integrity of the apical domain protein and indicating that the isolated apical domain retains much of the peptide binding ability of intact GroEL. Difference spectroscopy using far UV CD showed that no significant change occurs upon binding HD to ApEL, demonstrating that this peptide, similarly to helix A from the same protein (55, 56), binds to ApEL in a helical conformation (data not shown). Efficient binding of ML to ApEL was found to be slow and to require extended equilibration times in the range of 30 min. This relatively slow binding reaction could result from a slow association rate between ML and the apical domain or from a slow interconversion of apical domain conformations with differing affinities for ML.

In a second series of experiments, peptide binding to ApEL was also investigated using ESI-MS. Surprisingly, given the hydrophobic nature of substrate recognition by GroEL (reviewed in Refs. 11 and 14), measurable quantities of apical domain-peptide complexes could be detected by mass spectrometry under native conditions. Using ApEL at a concentration of 20 μM and ML at a concentration of ≥40 μM, the 1:1 complex between ML and the apical domain was partially preserved in the gas phase (Fig. 5*A*). However, the predominant mass species in the spectrum corresponded to uncomplexed protein and peptide. Similar observations were made for the complex between ApEL (20 μM) and HD (50 μM) under ESI-MS conditions (Fig. 5*B*). The dissociation of the complex in the gas phase accords with the hydrophobic nature of the noncovalent protein-ligand interactions, the strength of which is critically dependent on the presence of solvent. As hydrophobic interactions are predominantly solution dependent, there is little to sustain these interactions during the ESI process (57), where the removal of water is liable to cause the dissociation of apical domain-peptide complexes in the gas phase. Conversely, complexes that are stabilized by forces such as hydrogen bonds or electrostatic charge interactions are generally much better preserved in the gas phase (58, 59).

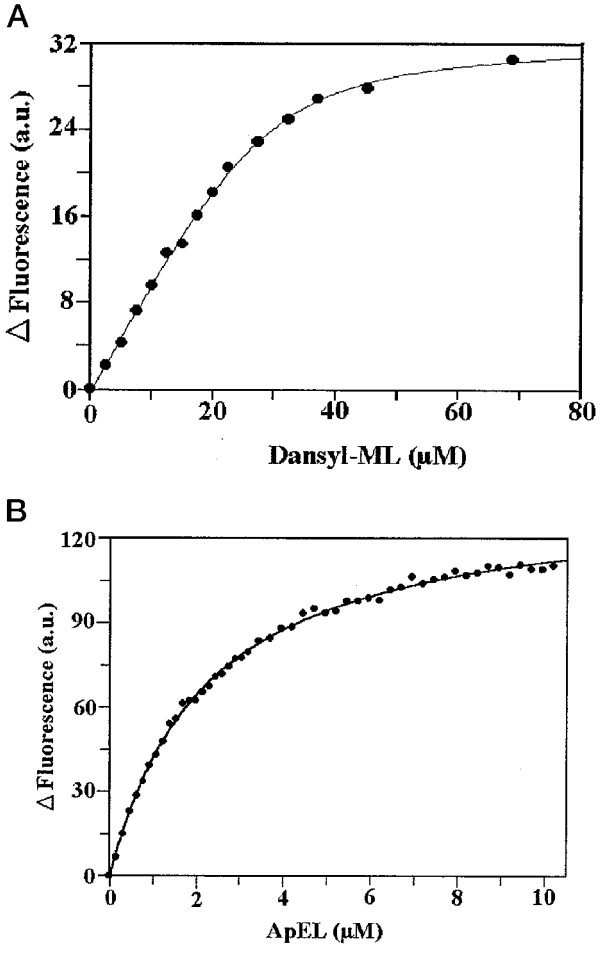

FIG. 4. **Fluorescence binding studies of ApEL with dansylated ML and HD peptides.** *A*, titration of ApEL with dansylated ML peptide. The change in fluorescence emission at 535 nm when ApEL (25 μM) is titrated with dansylated ML in buffer solution (Hepes (50 μM), DTT (2 mM), pH 7.5) at 20 °C is shown. The data have been fitted to a tight ligand binding equation giving a K_D of 2.7 ± 0.7 μM (*solid line*). *B*, titration of dansylated HD peptide with ApEL. The change in fluorescence emission at 500 nm is shown. Dansylated HD (3 μM) was dissolved in buffer solution (Hepes (50 μM), DTT (2 mM), pH 7.5) at 20 °C. The data have been fitted to a weak ligand binding equation giving a K_D of 2.2 ± 0.1 μM (*solid line*).

An interesting feature of this experiment is that the ESI-MS data show that only ApEL molecules in a folded or partially folded conformation are capable of gas-phase retention of bound peptides (Fig. 5, *A* and *B*). To estimate the percentage of the different apical domain conformations bound to ML and HD in the gas phase, the ESI-MS spectra were transposed onto a molecular mass profile (Fig. 6). To accomplish this, the *m/z* spectra were split into three regions encompassing the charge states associated with the folded (n = +8 to +11), partially folded (n = +13 to +17), and more highly unfolded (n = +20 to +28) populations identified above. Each region was then subjected individually to Maximum Entropy (39) processing, thus producing three mass profiles (Fig. 6). By comparison of the relative ion currents we estimate that ~26% (based on relative peak areas) of the most highly folded apical domain species, ~14% of the partially folded apical domain species, and 0% of the more highly unfolded apical domain species are detected bound to the ML peptide in the gas phase. There is also evidence for a trace (<2%) of a ternary complex between the highly folded apical domain and two molecules of ML. Very similar results were obtained also for the HD peptide (data not shown).

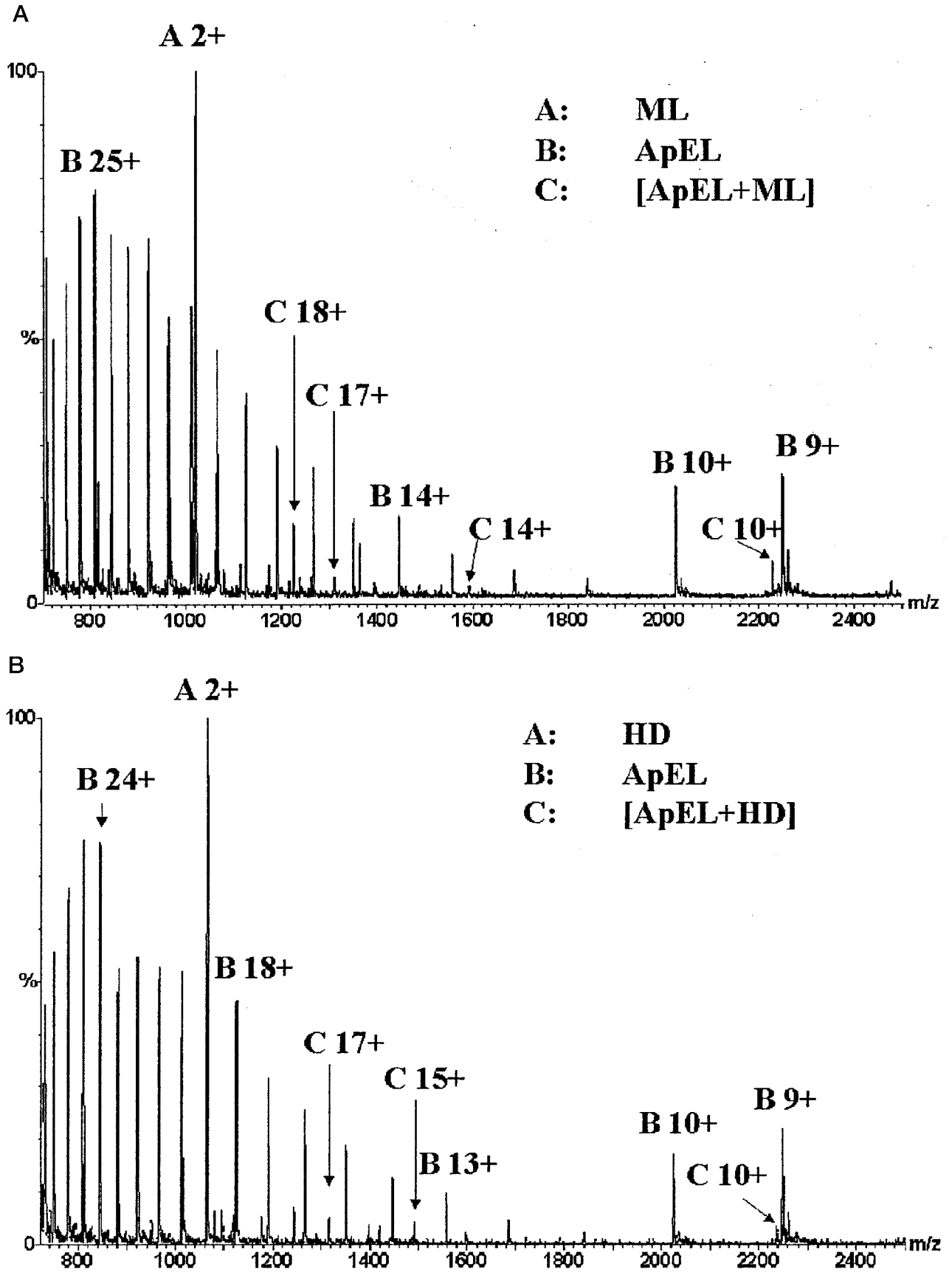

FIG. 5. **ESI-MS *m/z* spectra of noncovalently bound ApEL·peptide complexes.** The ESI-MS *m/z* spectra covering the range *m/z* 700–2500 of ApEL·peptide complexes analyzed under native conditions at pH 7.5 with an ionization source temperature of 30 °C and a sampling cone voltage of 30 V. *A*, ApEL (20 μM) and ML (40 μM) showing three components: *A* = ML; *B* = ApEL; and *C* = ApEL·ML complex. *B*, ApEL (20 μM) and HD (50 μM) showing three components: *A* = HD; *B* = ApEL; and *C* = ApEL·HD complex.

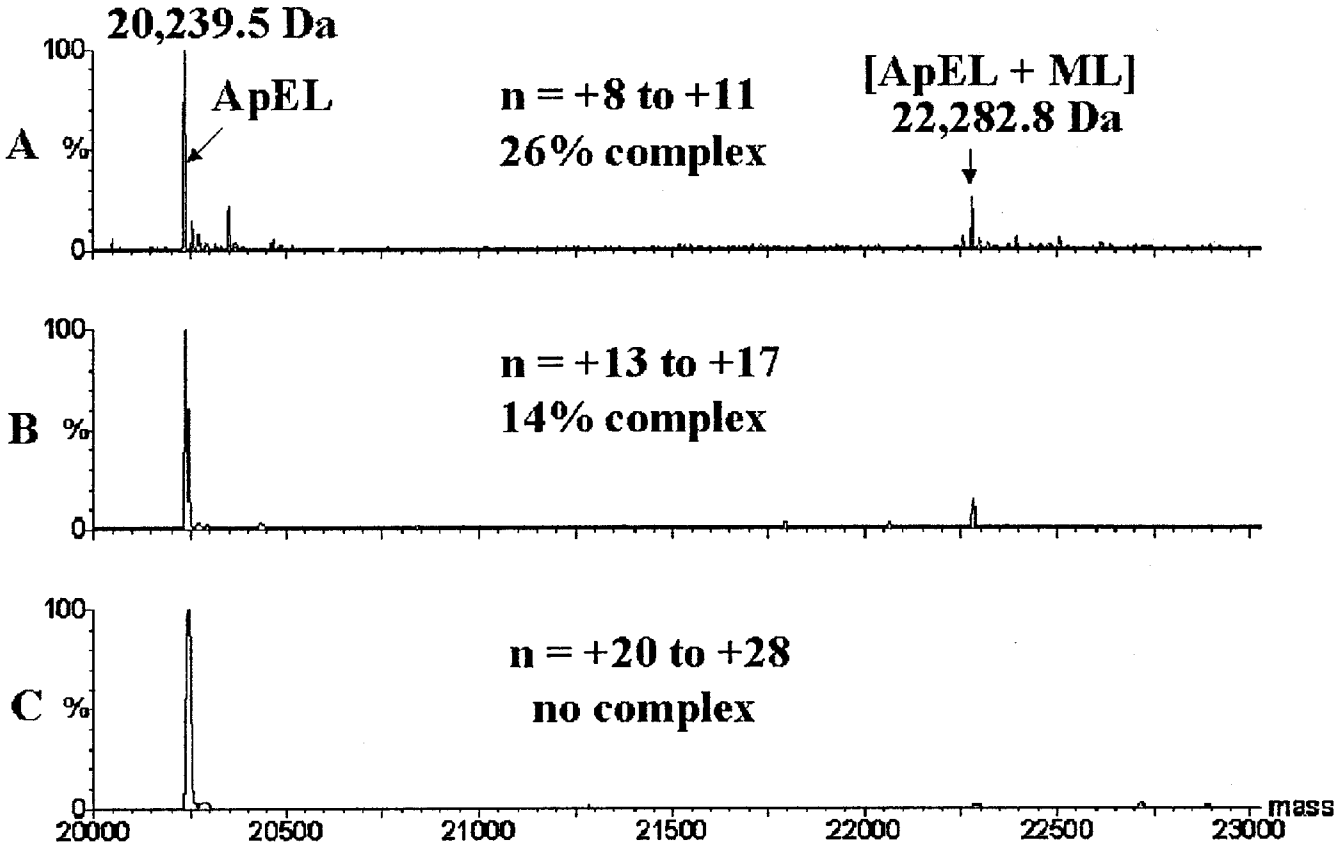

FIG. 6. **ESI-MS molecular mass profiles of noncovalently bound ApEL·peptide complexes.** The molecular mass (or zero charge) profiles generated by maximum entropy (39) processing techniques from the ESI-MS *m/z* spectrum of the mixture of ApEL and ML. *A*, the molecular mass profile generated from the *m/z* region covering the strongly folded apical domain (charge states $n = +8$ to $+11$). *B*, the molecular mass profile generated from the *m/z* region covering the partially folded apical domain (charge states $n = +13$ to $+17$). *C*, the molecular mass profile generated from the *m/z* region covering the more highly unfolded population (charge states +20 to +28). ApEL is observed in all populations, although the ApEL·ML complex is detected only in conjunction with the folded or partially folded states.

Simultaneous Binding of Mobile Loop and Helix D Peptides to GroEL Apical Domains—Although the binding site on the GroEL apical domain for ML and other peptides in an extended conformation has been mapped in detail by x-ray crystallography (19, 22, 51) there are currently no high resolution data highlighting the nature of the binding sites for helical substrates within the apical domain binding surface. NMR studies have suggested, however, that helices H and I are involved in the binding of helix A from rhodanese (56, 60) as well as intact proteins. To evaluate the extent of overlap of the binding sites for GroES and substrates in the apical domain of GroEL, a series of biochemical investigations was undertaken.

First, having established by fluorescence titrations that both ML and HD bind to ApEL (Fig. 4) with similar affinity, competition studies were undertaken using equilibrium fluorescence measurements. These were carried out by challenging complexes of ApEL or GroEL with dansylated peptides, with an excess of unlabeled competitor peptide. A decrease in the fluorescence intensity of the protein-dansylated peptide complexes would then be indicative of direct competition for peptide binding, whereas the fluorescence signal should be unperturbed in the absence of competition. The fluorescence emission spectrum of a preformed complex between ApEL (5 μM) and dansylated HD (5 μM) in the presence or absence of unlabeled ML (100 μM) is shown in Fig. 7*A*. No decrease in signal was observed when excess unlabeled ML was added to the ApEL·HD complex, suggesting that ML and HD are binding to distinct sites on the apical domain surface. The inability of ML to displace ApEL-bound dansylated HD is an important result as it is uncomplicated by the possibility of domain movements that can occur upon ligand binding to intact GroEL (10, 51). The preformed complex between intact GroEL (0.4 μM) and dansylated HD (3 μM) was also challenged with excess unlabeled ML (100 μM) (Fig. 7*B*). Again the results show that ML does not displace the bound dansylated HD. The protein-dansylated HD complexes show a slight increase in fluorescence emission in the presence of ML, which may suggest that the latter binds to a site close to dansylated HD, causing minor changes in the environment of the dansyl fluorophore.

The reverse competition experiment of challenging preformed protein-dansylated ML complexes with excess HD could only be performed reliably with intact GroEL, because the signal change accompanying the binding of dansylated ML to the apical domain is relatively small in magnitude (Fig. 4, *A* and *B*). The fluorescence emission spectrum of a preformed complex between GroEL (0.5 μM) and dansylated ML (20 μM) in the presence or absence of unlabeled HD (100 μM) is shown in Fig. 7*C*. Again the data reveal that ML and HD do not compete for binding to the GroEL surface. The instability of the peptide complexes in the gas phase precluded similar experiments using ESI-MS.

In a second series of experiments, a mutant of intact GroEL (EL N229C) was prepared in which every endogenous cysteine residue was exchanged for an alanine residue and a new cysteine was introduced at Asn^{229} (26). Cys^{229} is strategically well positioned at one end of the GroES binding groove formed by helices H and I in the apical domain of GroEL. A C-terminal maleimide-derivatized variant of the "strong binding peptide" (SBP-mal) that was shown elsewhere to bind into the same binding groove as the GroES mobile loop (19) was covalently

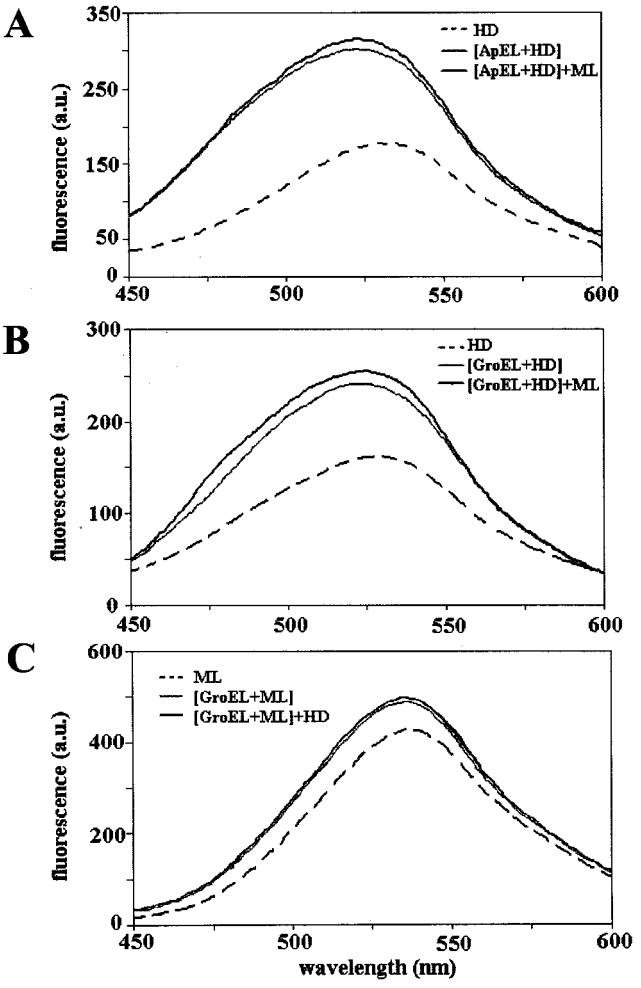

FIG. 7. **Fluorescence emission spectra from ApEL·peptide competition binding studies.** Fluorescence emission spectra from competition studies showing: *A*, the preformed complex of ApEL·HD from ApEL (5 μM) and dansylated HD (5 μM) in buffer (Hepes (50 μM), DTT (2 mM), pH 7.5) at 20 °C, in the presence and absence of ML (100 μM). *B*, the preformed complex of GroEL·HD from GroEL (0.4 μM) and dansylated HD (3 μM) in buffer (Hepes (50 μM), DTT (2 mM), pH 7.5) at 20 °C, in the presence and absence of ML (100 μM). *C*, the preformed complex of GroEL·ML from GroEL (0.5 μM) and dansylated ML (10 μM) in buffer (Hepes (50 μM), DTT (2 mM), pH 7.5) at 20 °C, in the presence and absence of HD (100 μM).

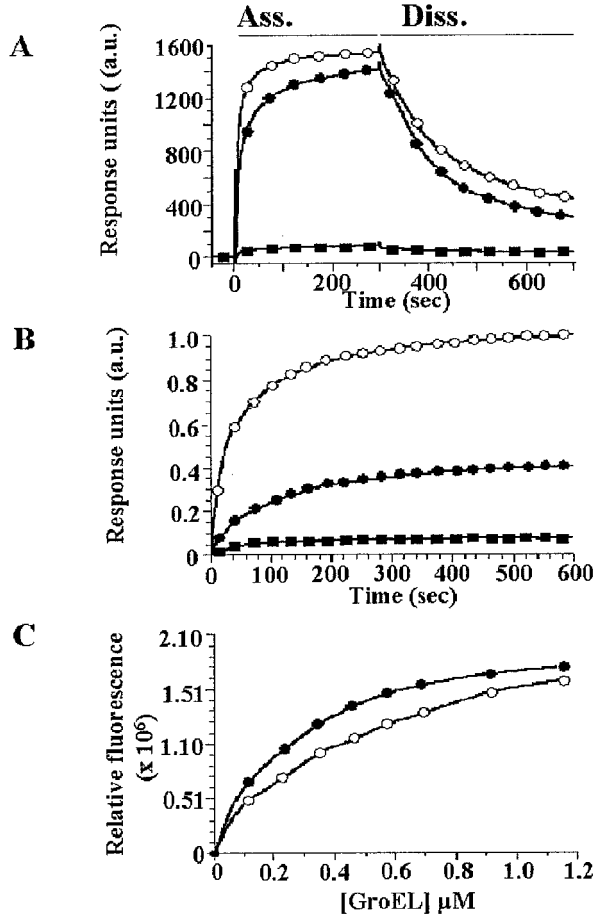

FIG. 8. **Binding assays comparing the binding characteristics of EL N229C and EL N229C-SBP with WT GroEL.** *A*, SPR-based binding of WT GroEL (*open circle*), EL N229C (*closed circle*), and EL N229C-SBP (*closed square*) to immobilized GroES. *B*, comparison of the ability of EL N229C and EL N229C-SBP to prevent rhodanese aggregation monitored by turbidity measurements at 320 nm. The traces show rhodanese alone (*open circles*), rhodanese in the presence of EL N229C-SBP (*closed circles*), and rhodanese in the presence of EL N229C (*closed squares*). *C*, titration of dansylated HD against EL N229C (*closed circle*) and EL N229C-SBP (*open circle*) monitored by fluorescence emission.

coupled to Cys^{229} to form EL N229C-SBP (see "Experimental Procedures"). Using a surface plasmon resonance-based binding assay to determine the GroES binding capacities of unmodified EL N229C and the peptide-bound mutant EL N229C-SBP, we found that unmodified EL N229C bound immobilized GroES 98C with an affinity similar to that of WT GroEL (26), whereas by contrast, the modified variant EL N229C-SBP was essentially incapable of cofactor binding (Fig. 8*A*). From these data we conclude that the covalently bound SBP peptide competes efficiently with the GroES mobile loop structures, and therefore that SBP immobilized at position Cys^{229} assumes the same binding mode relative to the intact GroEL 14-mer as the co-crystallized SBP peptide relative to the isolated GroEL apical domain (19). In agreement with these GroES binding data we find that EL N229C-SBP does not refold chemically denatured rhodanese, a stringently GroEL/GroES-dependent model substrate (data not shown). Unmodified EL N229C on the contrary refolds this model substrate with the same efficiency as WT GroEL (26).

Finally we investigated whether blocking the GroES-binding site by SBP in the apical domain of EL N229C impaired substrate binding. Comparison of the activity of EL N229C and EL N229C-SBP to prevent rhodanese aggregation showed that EL N229C-SBP still maintained a substantial (~70%) activity in substrate binding compared with the unmodified EL N229C (Fig. 8*B*). These data indicate that the binding sites of SBP and non-native proteins on the apical domain of GroEL overlap only partially. Rhodanese seems to interact with a more extensive region on the apical domain surface than that masked by SBP binding. This hypothesis is consistent with the fluorescence data shown above, suggesting that the peptides ML and HD, mimicking GroES and substrate, respectively, do not compete directly for the same binding site on the apical domain. In accord with this, further titration experiments showed that dansylated HD binds to EL N229C, but covalently bound SBP does not prevent dansylated HD binding to EL-N229C-SBP (Fig. 8*C*).

DISCUSSION

Although multiple charge state distributions have been reported for other proteins (*e.g.* Ref. 61), we show here for the first time that ApEL exhibits multiple charge state distributions under native conditions. These data are consistent with previous observations that ApEL denatures noncooperatively

(23, 46). The ESI-MS data presented here suggest that this behavior results from the denaturation of different conformational states within the ensemble as the temperature is raised, although noncooperative denaturation within a population cannot be ruled out. Consistent with this, thermal denaturation of the shorter apical domain construct 191–345 (46), in which there is no exchange of conformers, shows a single species at pH 7.0 and only a single set of resonances visualized by NMR (56).

The conformational dynamics observed in ApEL raise the intriguing possibility that substrate binding could occur by a mechanism akin to induced fit. In accord with this, only the partially folded and more highly folded populations bind the GroES and rhodanese substrate analogue peptides tightly, as judged by the survival of these complexes under ESI-MS conditions, yet stoichiometric binding is observed at a high concentration of peptides in solution. Furthermore, superposition of the x-ray structures of intact GroEL and of the various apical domain constructs with structures determined to date show that helices H and I, which are known to be involved in binding GroES and possibly also in the binding of some purported substrate analogues (15–20, 56), show distinct conformational variability. Such a model could account for the different substrates that bind to GroEL, including all α, all β, as well as mixed α/β proteins (13), and also a range of peptides with different secondary structural preferences (14, 38, 62, 63).

The ability of the apical domain constructs to bind two very different peptides, one a substrate mimic and one a GroES mimic, albeit with similar binding affinity, accords with similar affinity of the intact protein for its co-chaperone and substrate proteins (reviewed in Ref. 14). Moreover the change in fluorescence observed and the ability of both peptide complexes to survive, at least partially, in the gas phase, suggest that the binding sites for the two peptides are similar in nature. In accord with this, reduced α-lactalbumin, denatured pepsin, and the helical peptide A from rhodanese have all been shown to bind close to helices H and I of GroEL, in line with this substrate sharing a similar binding site to that of GroES (60). Hydrophobic interactions have long been known to play an important role in the binding of substrates to intact GroEL (reviewed in Refs. 11 and 14); consistent with this, only a minority of peptide molecules remains bound to ApEL in the gas phase. Nonetheless, a measurable and reproducible proportion of bound peptides is detected in the gas phase using ESI-MS, in agreement with the observation that electrostatic and hydrogen bonding also play some role in binding, as observed in the x-ray structures of the N-terminal protease cleavage tag (22) and the SBP peptide (19) to ApEL.

One of the most interesting results to emerge from this study is the observation that HD and ML do not compete for the same binding site in ApEL, despite having similar binding affinities for the protein. Similarly, no competition was observed by fluorescence emission data when the peptides were added to intact GroEL. These data, which are not influenced by the dynamic movements and cooperativity known to complicate binding experiments in intact GroEL, indicate that the binding sites on the apical domain surface, at least for these small peptides, are distinct. These binding sites are also at least partially distinct in intact GroEL, because HD is able to bind to EL N229C-SBP, albeit with slightly reduced affinity and, despite being unable to bind GroES, EL N229-SBP is able to bind rhodanese. Taken together, therefore, the data suggest that displacement of polypeptide from the apical domain surface by GroES can proceed via an indirect removal of the polypeptide-binding surfaces through the large conformational changes induced in the GroEL apical domains upon GroES and nucleotide binding, as well as by more direct ejection of the substrate protein into the central cavity upon GroES binding. The dynamic surface of the apical domain and of its partially unfolded substrates suggests that different proteins could bind to different sites on the apical domain surface and the manner by which the substrate is ejected into the central cavity could involve one or both of these mechanisms. Nonetheless, the conformational flexibility shown here directly for the apical domain surfaces using ESI-MS demonstrates that GroEL is exquisitely adapted to bind and fold its broad range of protein substrates.

The question remains, where might substrate proteins bind to the GroEL apical domain? Interestingly, although previous crystallographic studies of complexes with the apical domain have implicated helices H and I as the critical substrate-binding site, the peptide fragments bound in these cases show remarkable sequence similarity to the mobile loop of GroES (14). This raises the intriguing possibility that these peptides mimic GroES binding rather than substrate binding (14). Whereas there could be several binding sites for multivalent substrates within the dynamic apical domain surface, it is clear that significant conformational rearrangements would be required for a folded helix to bind between helices H and I, in a manner identical to that of the mobile loop of GroES. However, the data presented here suggest that HD of rhodanese binds in a helical conformation to a site distinct from that of the GroES mobile loop, in support of the view that intact substrate proteins could, most probably, bind to GroEL at multiple sites. Further experiments will be required to map the location of the binding site for HD and other substrates on the apical domain surface and to test further the relationship between GroES binding and substrate release during the GroEL functional cycle. Unfortunately the limited solubility of the HD sequence precluded studies of this kind, for example, using co-crystallization or NMR analysis. Nonetheless, the data presented here show clearly that substrate and GroES binding to GroEL could be distinct events, at least for some proteins, and highlight that there is still much to learn about the manner in which GroEL binds its substrate proteins and releases them in a manner commensurate for productive protein folding.

Acknowledgments—We thank Maureen Pitkeathly (Oxford Centre for Molecular Sciences) for preparing the synthetic peptides used in this study, Prof. Alan Fersht for kindly providing the coordinates of the GroEL apical domain 191–376 prior to publication, and Dr. Maire Convery for help with the x-ray structure.

REFERENCES

1. Hartl, F. U. (1996) *Nature* **381,** 571–579
2. Bukau, B., and Horwich, A. L. (1998) *Cell* **92,** 351–366
3. Hartl, F. U., and Hayer-Hartl, M. K. (2002) *Science* **295,** 1852–1858
4. Hemmingsen, S. M., Woolford, C., van der Vies, S. M., Tilly, K., Dennis, D. T., Georgopoulos, C. P., Hendrix, R. W., and Ellis, R. J. (1988) *Nature* **333,** 330–334
5. Grallert, H., and Buchner, J. (2001) *J. Struct. Biol.* **135,** 95–103
6. Kusmierczyk, A. R., and Martin, J. (2001) *Mol. Biotechnol.* **19,** 141–152
7. Ewalt, K. L., Hendrick, J. P., Houry, W. A., and Hartl, F. U. (1997) *Cell* **90,** 491–500
8. Houry, W. A., Frishman, D., Eckerskorn, C., Lottspeich, F., and Hartl, F. U. (1999) *Nature* **402,** 147–154
9. Braig, K., Otwinowski, Z., Hegde, R., Boisvert, D. C., Joachimiak, A., Horwich, A. L., and Sigler, P. B. (1994) *Nature* **371,** 578–586
10. Roseman, A. M., Chen, S. X., White, H., Braig, K., and Saibil, H. R. (1996) *Cell* **87,** 241–251
11. Feltham, J. L., and Gierasch, L. M. (2000) *Cell* **100,** 193–196
12. Sigler, P. B., Xu, Z., Rye, H. S., Burston, S. G., Fenton, W. A., and Horwich, A. L. (1998) *Annu. Rev. Biochem.* **67,** 581–608
13. Fenton, W. A., Kashi, Y., Furtak, K., and Horwich, A. L. (1994) *Nature* **371,** 614–619
14. Coyle, J. E., Jaeger, J., Grob, M., Robinson, C. V., and Radford, S. E. (1997) *Fold and Des.* **2,** R93–R104
15. Smote, A. L., Panda, M., Brazil, B. T., Buckle, A. M., Fersht, A. R., and Horowitz, P. M. (2001) *Biochemistry* **40,** 4484–4492
16. Wang, Q. H., Buckle, A. M., and Fersht, A. R. (2000) *J. Mol. Biol.* **304,** 873–881
17. Chatellier, J., Hill, F., and Fersht, A. R. (2000) *J. Mol. Biol.* **304,** 883–896
18. Chatellier, J., Hill, F., Foster, N. W., Goloubinoff, P., and Fersht, A. R. (2000) *J. Mol. Biol.* **304,** 897–910
19. Chen, L. L., and Sigler, P. B. (1999) *Cell* **99,** 757–768

20. Ma, J. P., Sigler, P. B., Xu, Z. H., and Karplus, M. (2000) *J. Mol. Biol.* **302,** 303–313
21. Braig, K., Adams, P. D., and Brunger, A. T. (1995) *Nat. Struct. Biol.* **2,** 1083–1094
22. Buckle, A. M., Zahn, R., and Fersht, A. R. (1997) *Proc. Natl. Acad. Sci. U. S. A.* **94,** 3571–3575
23. Weber, F., Keppel, F., Georgopoulos, C., Hayer-Hartl, M. K., and Hartl, F. U. (1998) *Nat. Struct. Biol.* **5,** 977–985
24. Weber, F., Keppel, F., Georgopoulos, C., Hayer-Hartl, M. K., and Hartl, F. U. (1999) *Nat. Struct. Biol.* **6,** 200–200
25. Pace, C. N., Vajdos, F., Fee, L., Grimsley, G., and Gray, T. (1995) *Protein Sci.* **4,** 2411–2423
26. Brinker, A., Pfeifer, G., Kerner, M. J., Naylor, D. J., Hartl, F. U., and Hayer-Hartl, M. (2001) *Cell* **107,** 223–233
27. Jancarik, J., and Kim, S. H. (1991) *J. Appl. Crystallogr.* **24,** 409–411
28. Leslie, A. G. W. (1992) *Joint CCP4 and ESF-EACMB Newsletter Protein Crystallography,* Vol. 26**,** Daresbury Laboratory, Warrington, UK
29. Collaborative Computational Project, N. (1994) *Acta Crystallogr. Sect. D* **50,** 760–763
30. Navaza, J. (1994) *Acta Crystallogr. Sect. A* **50,** 157–163
31. Pflugrath, J. W., Saper, M. A., and Quiocho, F. A. (1984) in *New Generation Graphics System for Molecular Modelling, Methods and Applications in Crystallographic Computing* (Hall, S., and Ashira, T., eds) Claredon Press, Oxford
32. Jones, T. A. (1978) *J. Appl. Crystallogr.* **15,** 268–272
33. Brunger, A. T. (1993) *XPLOR: A System for X-ray Crystallography and NMR,* Yale University Press, New Haven, CT
34. Jones, T. A. (1991) *Acta Crystallogr. Sect. A* **47,** 110–119
35. Adams, P. D., Pannu, N. S., Read, R. J., and Brunger, A. T. (1997) *Proc. Natl. Acad. Sci. U. S. A.* **94,** 5018–5023
36. Murshudov, G. N., Vagin, A. A., and Dodson, E. J. (1997) *Acta Crystallogr. Sect. D* **53,** 240–255
37. Ploegman, J. H., Drent, G., Kalk, K. H., Hol, W. G., Heinrikson, R. L., Keim, P., Weng, L., and Russell, J. (1978) *Nature* **273,** 245–249
38. Hutchinson, J. P., Oldham, T. C., Elthaher, T. S. H., and Miller, A. D. (1997) *J. Chem. Soc. Perkin Trans.* **2,** 279–288
39. Ferrige, A. G., Seddon, M. J., Green, B. N., Jarvis, S. A., and Skilling, J. (1992) *Rapid Commun. Mass Spectrom.* **6,** 707–711
40. Romano, R., Bayerl, T. M., and Moroder, L. (1993) *Biochim. Biophys. Acta* **1151,** 111–119
41. Ranson, N. A., Burston, S. G., and Clarke, A. R. (1997) *J. Mol. Biol.* **266,** 656–664
42. Rye, H. S., Roseman, A. M., Chen, S. X., Furtak, K., Fenton, W. A., Saibil, H. R., and Horwich, A. L. (1999) *Cell* **97,** 325–338
43. HayerHartl, M. K., Martin, J., and Hartl, F. U. (1995) *Science* **269,** 836–841
44. Weissman, J. S., Kashi, Y., Fenton, W. A., and Horwich, A. L. (1994) *Cell* **78,** 693–702
45. Boisvert, D. C., Wang, J., Otwinowski, Z., Horwich, A. L., and Sigler, P. B. (1996) *Nat. Struct. Biol.* **3,** 170–177
46. Zahn, R., Buckle, A. M., Perret, S., Johnson, C. M., Corrales, F. J., Golbik, R., and Fersht, A. R. (1996) *Proc. Natl. Acad. Sci. U. S. A.* **93,** 15024–15029
47. Brunger, A. T., Kurijan, J., and Karplus, M. (1987) *Science* **235,** 458–460
48. Raftery, M. J., and Geczy, C. L. (1998) *J. Am. Soc. Mass Spectrom.* **9,** 533–539
49. Kraunsoe, J. A. E., Aplin, R. T., Green, B. N., and Lant, G. (1996) *FEBS Lett.* **396,** 108–112
50. Landry, S. J., Taher, A., Georgopoulos, C., and van der Vies, S. M. (1996) *Proc. Natl. Acad. Sci. U. S. A.* **93,** 11622–11627
51. Xu, Z. H., Horwich, A. L., and Sigler, P. B. (1997) *Nature* **338,** 741–750
52. Hunt, J. F., Weaver, A. J., Landry, S. J., Gierasch, L. M., and Deisenhofer, J. (1996) *Nature* **379,** 37–45
53. Hlodan, R., Tempst, P., and Hartl, F. U. (1995) *Nat. Struct. Biol.* **2,** 587–595
54. Dessauer, C. W., and Bartlett, S. G. (1994) *J. Biol. Chem.* **269,** 19766–19776
55. Landry, S. J., and Gierasch, L. M. (1991) *Biochemistry* **30,** 7359–7362
56. Kobayashi, N., Freund, S. M. V., Chatellier, J., Zahn, R., and Fersht, A. R. (1999) *J. Mol. Biol.* **292,** 181–190
57. Robinson, C. V., Chung, E. W., Kragelund, B. B., Knudsen, J., Aplin, R. T., Poulsen, F. M., and Dobson, C. M. (1996) *J. Am. Chem. Soc.* **118,** 8646–8653
58. Smith, R. D., Bruce, J. E., Wu, Q., and Lei, Q. P. (1997) *Chem. Soc. Rev.* **26,** 191–202
59. Loo, J. A. (1997) *Mass Spec. Rev.* **16,** 1–23
60. Tanaka, N., and Fersht, A. R. (1999) *J. Mol. Biol.* **292,** 173–180
61. Konermann, L., and Douglas, D. J. (1997) *Biochemistry* **36,** 12296–12302
62. Chatellier, J., Buckle, A. M., and Fersht, A. R. (1999) *J. Mol. Biol.* **292,** 163–172
63. Brocchierei, L., and Karlin, S. (2000) *Protein Sci.* **9,** 476–486